

# MiR-365-3p is Involved in IL17-Mediated Asthma in Mouse Model

Weijia Wang

School of Life Science and Technology, Xi'an Jiaotong University

Ying Li

School of Life Science and Technology, Xi'an Jiaotong University

Xiaoyan Qu

School of Life Science and Technology, Xi'an Jiaotong University

Dong Shang

The First Affiliated Hospital, Xi'an Jiaotong University

Qiaohong Qin

Institute of Basic and Translational Medicine, Xi'an Medical University

Qutayba Hamid

The Research Institute of the McGill University Health Centre and Department of Medicine, McGill University

Xiaomin Dang

The First Affiliated Hospital, Xi'an Jiaotong University

Ying Chang (✉ [changyingcn@hotmail.com](mailto:changyingcn@hotmail.com))

School of Life Science and Technology, Xi'an Jiaotong University <https://orcid.org/0000-0001-9456-5333>

---

## Research

**Keywords:** HDM, miRNA, BALF, RNA

**Posted Date:** November 17th, 2020

**DOI:** <https://doi.org/10.21203/rs.3.rs-105229/v1>

**License:**  This work is licensed under a Creative Commons Attribution 4.0 International License.

[Read Full License](#)

---

## Abstract

**BACKGROUND** The IL-17 superfamily, which mediates cross-talk between the adaptive and innate immune systems, has been associated with severity of asthma. The role of miRNAs in the disease has been paid much attention. To explore the roles of IL-17 in asthma and the relationship between IL-17 and miRNAs, we used a model of severe asthma driven by chronic respiratory exposure to house dust mite (HDM) exposure in wild type and IL-17KO mice, followed with miRNA profiling assays and analysis.

**METHODS** Male and female C57BL/6 mice (6-8 weeks old) and IL-17KO mice (C57BL/6 background) were exposed to purified HDM extract intranasally for 5 days/week for 5 consecutive weeks. Sterile saline was used as the control. The parameters including airway responsiveness, inflammatory cells in bronchoalveolar lavage fluid (BALF), airway smooth muscle bundle, collagen deposition, and cytokine levels in BALF were examined. The miRNA profile of mouse lung tissue was analyzed by microarray assays. The dysregulation of miRNA related to IL-17 and asthma was validated by qRT-PCR. The in vitro cell culture experiment was performed to confirm the relationship between IL-17 and selected miRNA. The regulation of miRNA on predicted target gene was validated by administration of miRNA mimics.

**RESULTS** The expression of IL-17A significantly increased in wild type (WT) mice with HDM exposure compared to the control mice. IL-17 deficiency did not reduce airway hyper responsiveness (AHR) induced by HDM exposure. In comparison to HDM-exposed WT mice, BALF neutrophils in IL-17KO mice were significantly decreased. In WT mice, HDM exposure led to increased expression of IL-4 and KC, which was significantly decreased in IL-17KO mice. Furthermore, under HDM exposure, significantly less airway smooth muscle mass and collagen deposition was found in IL-17KO mice compared to WT mice. In the dysregulated miRNAs, the decreased expression of miR-365-3p in HDM-exposed WT mice was validated, and its expression recovered in IL-17KO mice. Furthermore, miR-365-3p was decreased in mouse alveolar epithelial cells by IL-17 treatment. The transfection of miR-365-3p mimics decreased the expression of predicted target gene ARRB2.

## Introduction

Asthma is a chronic inflammatory airway disease characterized by reversible airflow limitation. The pathogenesis of asthma is extremely complex. A variety of inflammatory cells and cellular components are involved in the airway inflammation of asthma. In addition to airway inflammation, airway remodeling is considered as the main pathological basis for irreversible airway obstruction and airway hyperresponsiveness<sup>1</sup>.

Th17 cytokines can induce the production of multiple chemokines, thereby recruiting neutrophils and macrophages to eliminate pathogens. Th17 cells are the intermediate link between innate immunity and adaptive immune response and are considered as potential inducers of autoimmunity and tissue inflammation <sup>2,3</sup>. Th17 cells have been associated with autoimmune diseases such as experimental autoimmune encephalitis (EAE) and rheumatoid arthritis (RA). Recent studies showed that Th17 cells and

cytokines are involved in the pathogenesis of asthma<sup>4</sup>. In previous studies, we found that Th17 cytokines including IL-17A / F and IL-22 can induce the migration and proliferation of airway smooth muscle cells (ASMCs)<sup>5,6</sup>. We also found that IL-17A / F can stimulate ASMCs to produce a variety of cytokines and chemokines, of which CXCL1,2 and 3 are the most secreted chemokines, and the supernatant of IL-17A / F stimulated cells can also promote the chemotaxis of ASMCs<sup>7</sup>. The above research results from *in vitro* experiments showed that Th17 cytokines may participate in the formation of airway remodeling by promoting the chemotaxis, proliferation and secretion of ASMC.

MiRNA is a type of endogenous non-coding RNA with regulatory functions found in eukaryotes, and its size is about 20–25 nucleotides in length. Recent studies have shown that miRNAs are involved in a variety of regulatory pathways and play a key role in a variety of diseases, including cancer, viral infections and inflammatory diseases of the lungs<sup>8</sup>. In recent years, the role of miRNAs in the development of asthma has received increasing attention. Recent publications confirmed the crucial regulatory role of miRNAs in the pathogenesis of asthma<sup>9</sup>. Interestingly, IL-17 can regulate the release of inflammatory factors and chemokines by astrocytes in experimental autoimmune encephalomyelitis through miRNA, which in turn aggravates the disease<sup>10</sup>. This provides a clue for elucidating the mechanism of IL-17 regulating severe asthma.

To explore the roles of IL-17 in asthma and the relationship between IL-17 and miRNAs, we used a model of severe asthma in wild type and IL-17 deficient mice, followed with miRNA profiling assays and analysis. We demonstrated that IL-17 plays an important role in the pathogenesis of severe asthma by the recruitment of neutrophils, the induced expression of IL-4, IL-5, IL-13 and KC, and the promotion of airway remodeling. In the dysregulated miRNAs, the expression of miR-365-3p was decreased in HDM-exposed WT mice, and its expression was resumed in IL-17KO mice. The further *in vitro* studies validated the regulatory role of miR-365-3p on the target gene ARRB2. Our studies demonstrated for the first time the IL-17 related miRNAs in asthmatic mice, which may provide experimental evidence for the IL-17 and miRNA targeting therapy of asthma.

## Methods

### Animals

C57BL/6 female mice (6-8 wk) were purchased from Charles River (Montreal, Canada). IL-17KO mice were prepared as previously described<sup>11</sup>. All animals were treated and maintained under a protocol approved by the Animal Care Committee of McGill University, following guidelines set by the Canadian Council on Animal Use and Care.

### Antigen Administration

Wild type and IL-17KO mice were exposed to purified HDM extract (Greer Laboratories, Lenoir, NC) intranasally (25 mg of protein in 10 ml of saline) for 5 days/week for five consecutive weeks. The

equivalent volume of saline was used as the control. Each group contained 10 mice. The mice were killed at 24 h after the last exposure.

### **Preparation of bronchoalveolar lavage fluid**

The lungs were lavaged using a cannula inserted in the trachea and the lungs were instilled with 0.5 ml PBS. Cytospins were prepared at a density of  $0.5 \times 10^6$  cells/ml. Differential cell counts were performed using standard morphological criteria on Hema-Gurr-stained cytospins (500 cells/sample) (Merck, Darmstadt, Germany).

### **Bronchoalveolar lavage cytokine analysis**

Aliquots of cell-free bronchoalveolar lavage fluid (BALF) were frozen in liquid N<sub>2</sub> and stored at -80°C. The levels of IL-4, IL-5, IL-13, IL-10, TNF-α, IFN-γ and KC in BALF were analyzed by the Bio-plex system (Bio-Rad, Mississauga, Ontario, Canada) performed in the Goodman Cancer Centre Transgenic Core Facility, McGill University, Canada.

### **Immunohistochemistry staining**

The immunohistochemistry staining for IL-17A (Santa Cruz Biotechnology, Santa Cruz, CA, USA) and α-SMA (Santa Cruz Biotechnology) was performed on paraffin-embedded mouse lung tissue sections as previously described <sup>12</sup>.

### **miRNA expression array**

Equal amount of RNA sample from each mice of different groups was pooled respectively for miRNA profiling assay using μParaflo®Microfluidic Biochip miRNA microarray (LC Sciences, Houston, USA).

### **Real-time quantitative RT-PCR**

Independent assays were performed using quantitative reverse transcription PCR (qRT-PCR) on all mouse samples for individual miRNA (miR-207, miR-5112, miR-2861, miR-340-5p, miR-6238, miR-181c-5p, miR-6239, miR-365-3p and miR-133b-3p) (Qiagen, Hilden, Germany) and predicted target genes (FASL, TRAF3, ARRB2, Sgk1, PIK3R3, ADAM10 and ADM) (Bio-rad, Foster City, USA). Data were presented relative to U6 for miRNA and β-actin for target genes based on calculations of  $2^{(-\Delta\Delta Ct)}$ . The primer sequences for target genes were listed in Table 1. Statistical significance was defined as p < 0.05 as measured by the t-test using GraphPad Prism 5 software (GraphPad, San Diego, USA).

**Table 1.** The sequence of primers for real-time PCR

Gene	Sequence (5'-3')	Direction
FASL	GAACTCCGTGAGCCAACCC	Forward
	CCAGAGATCAGAGCGGTTCC	Reverse
TRAF3	GCGTGCCAAGAAAGCATCAT	Forward
	CCTCTGCCTTCATTCCGACA	Reverse
ARRB2	ACACGCCACTTCCTCATGTC	Forward
	TCTTCTTGACGGTCTGGCA	Reverse
Sgk1	ATCCTGACCAAGCCGGACC	Forward
	AAAATCGTCAGGCCCATCCTT	Reverse
PIK3R3	AAGATGCAGAGTGGTACTGGG	Forward
	CCTGCATTTCGTTGAGGCA	Reverse
ADAM10	ACACCAAAAACACCAGCGTG	Forward
	GGAAGTGTCCCTCTTCATT CGT	Reverse
ADM	ATTGGGTTCACTCGCTTCCT	Forward
	GCTGGATGCTTGAGTTCCT	Reverse
b-actin	GATGCCCTGAGGCTTTTCC	Forward
	TCTTACGGATGTCAACGTACAC	Reverse

### Mouse lung epithelial cell culture.

Mouse lung epithelial cells (MLE-12 cells), a distal bronchiolar and alveolar epithelial cell line (ATCC, Manassas, VA)<sup>13</sup>, were cultured in HITES medium (50:50, DMEM-Ham's F-12) supplemented with 2% FBS, 2 mM L-glutamine, 10 mM HEPES, 1:100 insulin/transferrin/selenium supplement (Sigma, St. Louis, MO, USA) and antibiotics. After 24 h of starvation with HITES medium containing 0.1% FBS, cells were cultured with different concentrations (0, 1, 10 and 100ng/ml) of mouse recombinant IL-17A (R&D Systems, Minneapolis, USA) for 24h, and the expression of miR-365-3p was examined by qRT-PCR. Alternatively, the mimic (100nM) or inhibitor (100nM) of miR-365-3p was transfected into the cells by using X-tremeGENE siRNA Transfection Regent (Roche, Penzberg, Upper Bavaria, Germany) in Opti-MEM (Gibco, Grand Island, NY, USA) for 24h, the expression of ARRB2 was examined by qRT-PCR and Western blot.

### Luciferase reporter assay

Sense and antisense sequences corresponding to a 406-bp fragment from the 3'UTR of ARRB2 with the predicted binding and mutated sites (position 236–243) were amplified from cDNAs of mouse lung tissue by using primers containing the SacI restriction site in the sense oligo and XbaI restriction site in the antisense oligo (Sense: 5'-ATCGAGCTCCTGTCCACCCGAGATACAC-3'; Antisense: 5'-AGCTCTAGAGGTACCCTGCAGATGTAGAA-3'; GenePharma, Shanghai, China). To construct luciferase reporter plasmids for ARRB2, the annealed synthetic oligos were cloned downstream to the firefly luciferase into SacI-XbaI double digested pmirGLO Dual-Luciferase miRNA target expression vector (Promega, WI, USA). For the luciferase reporter assay, 293-T cells (ATCC) were co-transfected with 250 ng of luciferase reporter plasmid harboring the wild type/mutant binding sites of ARRB2 respectively along with 25nM mimic control/miR-365-3p mimic using X-tremeGENE siRNA Transfection Reagent (Roche) in Opti-MEM (Gibco). After 48h of transfection, cells were washed in PBS and lysed in Reporter lysis buffer (Promega), and luciferase activity was measured in a FlexStation 3 microplate reader (Molecular Devices, Sunnyvale, CA, USA) using the Dual-Luciferase reporter assay kit (Promega) according to the manufacturer's instructions. Firefly luciferase activity was normalized to Renilla luciferase activity, and relative luciferase activity was calculated taking firefly luciferase activity of empty pmirGLO transfected cells as 100 percent.

### **Western Blot**

The protein samples of mouse lung tissue or MLE-12 cells were loaded (5 µg) on a 10% acrylamide SDS-PAGE gel (Bio-Rad, Hercules, USA) for protein separation, followed by transfer to PVDF membranes (Bio-Rad). The blots were then blocked with 1% BSA in 0.1% Tween 20/TBS for 1 h at room temperature and then incubated overnight at 4°C with antibodies specific for ARRB2 (Novus Biologicals, Centennial, CO, USA). After washing with 0.1% Tween 20 in TBS, the membranes were incubated with a 1: 3000 dilution of goat anti-rabbit IgG HRP (EMD Millipore Corp, Burlington, Massachusetts, USA) in 1% solution of powdered milk in TBS/0.1% Tween 20. The membranes were exposed to ECL solution (Bio-Rad) and imaged by chemiluminescence (Clinx Science Instrument, Shanghai, China).

### **Statistical analysis**

Statistical analysis for expression of miRNAs and mRNAs by qRT-PCR in mouse lung tissue was performed by unpaired test. The paired t-test was performed for cell culture experiments. Probability values of  $P < 0.05$  were considered significant. Data analysis was performed by using the GraphPad Prism 5 software (GraphPad, San Diego, CA, USA).

## **Results**

### **The important role of IL-17 in the pathogenesis of severe asthma model mice**

To investigate the role of IL-17 in severe asthma, IL-17 expression in the lung tissue of severe asthmatic mice was first examined. The level of IL-17 in bronchoalveolar lavage fluid (BALF) in the model group were significantly higher than those in the control group  $\square P<0.01$ , Figure 1 $\square$ . Meanwhile, IL-17

immunohistochemical staining showed that the positive cells expressing IL-17 in the model group increased. From the observation of cell morphology, most of the IL-17 expressing cells are macrophages and lymphocytes (Figure 1).

The results of the counts of various types of inflammatory cells in BALF showed that compared with the WT control mice, the number of various types of cells in the WT model group mice was significantly increased ( $P<0.05$ ,  $P<0.01$ ; Figure 2A). Compared with the WT model group, the total cell number, macrophages, neutrophils and lymphocytes in the IL-17KO model group were significantly reduced ( $P<0.05$ ; Figure 2A). Observation of mouse lung tissue sections showed that compared with WT model mice, IL-17KO model mice had significantly thinner airway wall, airway smooth muscle and submucosal layer. The inflammatory cell infiltration was significantly reduced (Figure 2B).

The cytokine levels in BALF were detected by ELISA. Compared with the WT control group, the Th2 cytokine levels including IL-4, IL-5 and IL-13 in the WT model group were significantly increased. In addition, the level of pro-inflammatory cytokine KC was also significantly increased in the WT model group. Compared with the WT model group, the levels of IL-4, IL-5, IL-13 and KC in the IL-17KO model group were significantly reduced (Figure 3).

The immunohistochemical staining of airway smooth muscle cells on mouse lung tissues showed that the airway smooth muscle area in WT severe asthmatic mice was significantly increased, while that in IL-17KO model mice was significantly reduced (Figure 4A). Similarly, the collagen deposition in the lung tissue of IL-17KO model mice was also significantly reduced (Figure 4B).

The overall results suggested that IL-17 is involved in both inflammation and airway remodeling in severe asthma.

### **miRNA expression profile in mouse lung tissue**

The miRNA expression profiles in the lung tissues of each group of mice were detected by using miRNA microarray assay. The results showed that the expression of 31 miRNAs in WT model mice changed by more than 1.5 times compared with WT control group, of which 26 miRNAs increased, 5 miRNAs decreased (Table 1). While the expression of miR-5112, miR-207, miR-2861, miR-340-5p, miR-6238, miR-181c-5p, miR-6239, miR-365-3p and miR-133b-3p was equivalent between IL-17KO model and IL-17KO control mice (Table 2). We further verified the expressions of the above-mentioned differentially expressed miRNAs in mouse lung tissue, the results showed that the expressions of miR-340-5p and miR-365-3p were significantly different between WT control and WT model group, while only miR-365-3p appeared equivalent expression between IL-17KO control and IL-17KO model group (Figure 5).

**Table 1.** Differentially expressed miRNAs in wild-type severe asthma model ( $\geq 1.5$ -fold)

Upregulation			Downregulation		
miRNA	Fold change	P-value	miRNA	Fold change	P-value
mmu-miR-5112	3.67	2.69E-03	mmu-miR-3107-5p	0.62	2.70E-03
mmu-miR-155-5p	2.46	2.09E-03	mmu-miR-1186b	0.58	1.82E-03
mmu-miR-207	2.45	9.01E-04	mmu-miR-133a-3p	0.58	5.24E-05
mmu-miR-223-3p	2.00	4.46E-03	mmu-miR-365-3p	0.57	4.38E-05
mmu-miR-3473e	2.00	3.55E-04	mmu-miR-133b-3p	0.54	2.63E-05
mmu-miR-148a-3p	1.98	2.96E-04			
mmu-miR-2861	1.95	1.51E-03			
mmu-miR-494-3p	1.92	1.30E-04			
mmu-miR-2137	1.90	2.48E-03			
mmu-miR-340-5p	1.86	7.38E-03			
mmu-miR-3473b	1.83	7.20E-06			
mmu-miR-132-3p	1.81	9.04E-05			
mmu-miR-139-5p	1.76	2.62E-04			
mmu-miR-1224-5p	1.74	4.29E-03			
mmu-miR-142-3p	1.71	1.87E-03			
mmu-miR-378c	1.71	1.18E-03			
mmu-miR-378a-3p	1.68	3.25E-03			
mmu-miR-7a-5p	1.65	5.10E-03			
mmu-miR-5126	1.64	1.88E-03			
mmu-miR-6238	1.61	7.13E-03			
mmu-miR-378d	1.58	3.57E-03			
mmu-miR-181c-5p	1.57	5.95E-03			
mmu-miR-21a-5p	1.57	2.17E-03			
mmu-miR-5117-5p	1.57	4.55E-03			
mmu-miR-378b	1.56	2.74E-05			
mmu-miR-6239	1.55	2.14E-03			

**Table 2.** Equivalently expressed miRNAs in IL-17KO model and IL-17KO control mice

miRNA	Fold change			
	WT Saline	WT HDM	IL-17KO Saline	IL-17KO HDM
mmu-miR-5112	1.00	3.67	0.80	0.90
mmu-miR-207	1.00	2.45	0.70	0.78
mmu-miR-2861	1.00	1.95	0.84	0.99
mmu-miR-340-5p	1.00	1.86	1.00	1.21
mmu-miR-6238	1.00	1.61	0.66	0.94
mmu-miR-181c-5p	1.00	1.57	2.21	0.72
mmu-miR-6239	1.00	1.55	1.11	1.02
mmu-miR-365-3p	1.00	0.57	1.04	1.35
mmu-miR-133b-3p	1.00	0.54	1.27	0.83

### Target gene prediction and verification of expression level

The target genes of miR-365-3p were predicted by the TargetscaN database. Among these predicted target genes, TRAF3, ARRB2, Sgk1, PIK3R3, ADAM10 and ADM are the ones that have been reported to be related to asthma. The expression of these genes in mouse lung tissue was tested. The results showed that the expression of ARRB2 was significantly higher in WT control group compared with WT model group, and its expression was equivalent between IL-17KO control and IL-17KO model group (Figure 6A). The expression of ARRB2 in the mouse lung tissue at protein level was detected by western blot (Figure 6B).

### Verification of the regulation of miR-365-3p on target gene

Since the reductive level of miR-365-3p was found in the WT model group and recovered in the IL-17KO mice, we investigated whether miR-365-3p expression could be affected by IL-17 stimulation in the mouse alveolar epithelial cells. The results showed that the expression of miR-365-3p was significantly reduced by the stimulation of different concentrations of IL-17 (Figure 7A).

To validate the targeting role of miR-365-3p on ARRB2, the luciferase reporter assay was performed. As shown in Figure 7B, the transfection of miR-365-3p mimic could significantly reduce the luciferase activity, suggesting ARRB2 is the target gene of miR-365-3p. Furthermore, miR-365-3p mimic could reduce the expression of ARRB2 in MLE-12 cells, while the inhibitor significantly increased the expression level at both mRNA (Figure 7C) and protein level (Figure 7D).

## Discussion

Our previous studies and other studies have demonstrated that IL-17 may play an important role in asthma. In the present study, we first established the severe asthma model by using the wild type and IL-17KO mice to investigate the role of IL-17 in the pathogenesis of severe asthma. The results showed that in the severe asthma models, IL-17 deficiency could reduce the infiltration of inflammatory cells in the lung tissue, the level of Th2 cytokines, the airway smooth muscle mass, and collagen deposition, indicating that IL-17 plays an important role in multiple parts of severe asthma. These results support the previous *in vitro* findings.

MicroRNAs play important regulatory roles in cell differentiation, cell cycle, and apoptosis<sup>8</sup>. Due to the role of multiple gene regulation, miRNAs have received much attention as biomarkers and target for novel therapeutics. Emerging studies explored the roles of miRNAs in severe asthma<sup>14</sup>. Different miRNAs play roles in biological mechanisms underlying Th2 and macrophage polarization, type 2 innate lymphoid cell biology regulation, steroid-resistant asthma phenotype, airway smooth muscle dysfunction and impaired anti-viral innate immune. We hypothesized that IL-17 may regulate asthma through miRNA. Thus, we further performed miRNA array assay in both WT and IL-17KO mice with or without HDM challenging.

Compared with WT model mice, a total of 31 miRNAs were dysregulated in WT control mice. Among these miRNAs, miR-155-5p<sup>15</sup>, miR-148a-3p<sup>16</sup>, miR-494-3p<sup>17</sup>, miR-142-3p<sup>18</sup>, miR-378d<sup>19</sup>, miR-181c-5p<sup>20</sup>, miR-21a-5p<sup>21</sup>, miR-3107-5p<sup>22</sup> and miR-133a-3p<sup>23</sup> have been reported to be dysregulated in asthma. Finally, the expression of miR-365-3p was validated to be significantly lower in WT model mice, while equivalent between IL-17KO control and IL-17KO model mice, suggesting that miR-365-3p is related to IL-17 in the severe asthma model.

MiR-365-3p was found up-regulated in multiple sclerosis and down-regulated in psoriasis<sup>24</sup>. Its level in serum was reported to be associated with the IL-17<sup>25</sup>. Depending on the different types of cancer, miR-365-3p could act as either an inhibitor or a promoter in tumorigenesis<sup>26,27</sup>. Besides the controversial role in tumorigenesis, miR-365 is considered to be a potential biomarker to identify the phenotypes of asthma, because the expression of miR-365 in severe asthma is lower than mild type<sup>28</sup>. Furthermore, miR-365-3p was up-regulated during the development of bronchopulmonary dysplasia of rat model<sup>29</sup>. To our knowledge, our study reported for the first time the dysregulation of miR-365-3p in the mouse severe asthma model. We found miR-365-3p is highly expressed in IL-17KO mice and negatively related with IL-17 expression, therefore, miR-365-3p is likely to play an anti-inflammatory role in asthma.

We further predicted the target genes of miR-365-3p, the expression of target genes TRAF3, ARRB2, Sgk1, PIK3R3, ADAM10 and ADM was examined. The dysregulation of ARRB2 in WT model mice and the recovery in IL-17KO model mice were validated at both mRNA and protein levels. Furthermore, the targeting role of miR-365-3p on ARRB2 was confirmed by both luciferase reporter assay and transfection of mimic and inhibitor of miR-365-3p.

ARRB2 (beta-arrestin-2) is an intercellular molecular regulating G protein-coupled receptor function and associating with receptor internalization<sup>30</sup>, which is involved in CD4<sup>+</sup> T cells migration, Th2 cell chemotaxis, and inflammatory cytokine production in asthma<sup>31,32</sup>. Increased ARRB2 expression in OVA-challenged mice and repressed inflammatory responses in ARRB2 deficiency mice<sup>33</sup> both demonstrated the key role of ARRB2 in the pathogenesis of asthma. Our study showed the association of IL-17 and ARRB2 via the regulation of miR-365-3p in the severe asthma mouse model.

Overall, through miRNAs expression profiling in WT and IL-17KO severe asthma mouse models, we identified the association of miR-365-3p of IL-17 in severe asthma. The further analysis of target genes indicated ARRB2 is regulated by miR-365-3p. Thus IL-17 may play important roles through miR-365-3p/ARRB2 in severe asthma, which may provide the clue for the potential therapeutic targets.

## Conclusions

Taken together, these findings suggest that IL-17 plays an important role in the inflammatory response and airway remodeling, and miR-365-3p may be a key miRNA involved in this regulation.

## Abbreviations

**IL** interleukin

**HDM** house dust mite

**KO** knock out

**BALF** bronchoalveolar lavage fluid

**qRT-PCR** quantitative reverse transcriptase polymerase chain reaction

**WT** wild type

**AHR** airway hyper responsiveness

**KC** keratinocyte chemoattractant

**ARRB2** beta arrestin 2

**EAE** experimental autoimmune encephalitis

**RA** rheumatoid arthritis

**CXCL** C-X-C motif chemokine ligand

**ASMC** airway smooth muscle cells

**PBS** phosphate-buffered saline

**TNF- $\alpha$**  tumor necrosis factor- $\alpha$

**IFN- $\gamma$**  interferon- $\gamma$

**$\alpha$ -SMA**  $\alpha$ -smooth muscle actin

**FASL** Fas-ligand

**TRAF3** TNF receptor associated factor 3

**Sgk1** serum/glucocorticoid regulated kinase 1

**PIK3R3** phosphoinositide-3-kinase regulatory subunit 3

**ADAM10** ADAM metallopeptidase domain 10

**ADM** Adrenomedullin

**DMEM** Dulbecco's modified Eagle's medium

**HEPES** N-2-hydroxyethylpiperazine-N-2-ethanesulfonic acid

**HITES** hydrocortisone, insulin, transferrin, estrogen, and selenium

**UTR** untranslated region

**MLE-12** murine lung epithelial-12

**SDS** sodium dodecyl sulfate

**PAGE** polyacrylamide gel electrophoresis

**PVDF** polyvinylidene difluoride

**BSA** bovine serum albumin

**TBS** Tris-buffered saline

**HRP** horseradish peroxidase

**ECL** enhanced chemiluminescence

**ELISA** enzyme-linked immunosorbent assay

## Declarations

## **Ethics approval and consent to participate**

This study was approved by the Animal Care Committee of McGill University. All animals were treated and maintained under a protocol in accordance with the institutional ethical requirements and supported by the Canadian Council on Animal Use and Care.

## **Consent for publication**

Not applicable

## **Availability of data and material**

Not applicable

## **Funding**

This study was supported by the National Natural Science Foundation of China (31501044), Natural Science Basic Research Plan in Shaanxi Province of China (2020JM-002), International Cooperation, Exchange Program of Science and Technology of Shaanxi Province (2020KW-046), and The Science and Technology Innovation Base-Open and Sharing Platform of Science and Technology Resource Project of Shaanxi Province (2019PT-26).

## **Competing interests**

There is no competing financial interest.

## **Authors' contributions**

WW performed qRT-PCR, western blotting and analyzed the results. YL coordinated the animal experiments. XQ cultured the cells, DS coordinated the histochemistry staining. QQ coordinated the animal experiments. QH revised the manuscript. XD performed ELISA. YC designed the study, performed the animal experiments and drafted the manuscript. All authors read and approved the final manuscript.

## **Acknowledgements**

Not applicable

## **References**

1. Girodet PO, Ozier A, Bara I, Tunon de Lara JM, Marthan R, Berger P. Airway remodeling in asthma: new mechanisms and potential for pharmacological intervention. *Pharmacol Ther* 2011;130:325-37.
2. Bettelli E, Korn T, Oukka M, Kuchroo VK. Induction and effector functions of T(H)17 cells. *Nature* 2008;453:1051-7.

3. Kramer JM, Gaffen SL. Interleukin-17: a new paradigm in inflammation, autoimmunity, and therapy. *J Periodontol* 2007;78:1083-93.
4. Gurczynski SJ, Moore BB. IL-17 in the lung: the good, the bad, and the ugly. *American journal of physiology Lung cellular and molecular physiology* 2018;314:L6-L16.
5. Chang Y, Al-Alwan L, Risse PA, et al. TH17 cytokines induce human airway smooth muscle cell migration. *The Journal of allergy and clinical immunology* 2011;127:1046-53 e1-2.
6. Chang Y, Al-Alwan L, Risse PA, et al. Th17-associated cytokines promote human airway smooth muscle cell proliferation. *FASEB J* 2012;26:5152-60.
7. Al-Alwan LA, Chang Y, Baglione CJ, et al. Autocrine-regulated airway smooth muscle cell migration is dependent on IL-17-induced growth-related oncogenes. *The Journal of allergy and clinical immunology* 2012;130:977-85 e6.
8. Oglesby IK, McElvaney NG, Greene CM. MicroRNAs in inflammatory lung disease—master regulators or target practice? *Respiratory research* 2010;11:148.
9. Specjalski K, Niedoszytko M. MicroRNAs: future biomarkers and targets of therapy in asthma? *Current opinion in pulmonary medicine* 2020;26:285-92.
10. Liu X, He F, Pang R, et al. Interleukin-17 (IL-17)-induced microRNA 873 (miR-873) contributes to the pathogenesis of experimental autoimmune encephalomyelitis by targeting A20 ubiquitin-editing enzyme. *The Journal of biological chemistry* 2014;289:28971-86.
11. Nakae S, Komiyama Y, Nambu A, et al. Antigen-specific T cell sensitization is impaired in IL-17-deficient mice, causing suppression of allergic cellular and humoral responses. *Immunity* 2002;17:375-87.
12. Chang Y, Nadig J, Boulais N, et al. CD8 positive T cells express IL-17 in patients with chronic obstructive pulmonary disease. *Respiratory research* 2011;12:43.
13. Rahman I. Oxidative stress in pathogenesis of chronic obstructive pulmonary disease: cellular and molecular mechanisms. *Cell biochemistry and biophysics* 2005;43:167-88.
14. Maneechoteswan K. Role of microRNA in severe asthma. *Respiratory investigation* 2019;57:9-19.
15. Zhou H, Li J, Gao P, Wang Q, Zhang J. miR-155: A Novel Target in Allergic Asthma. *International journal of molecular sciences* 2016;17.
16. Specjalski K, Jassem E. MicroRNAs: Potential Biomarkers and Targets of Therapy in Allergic Diseases? *Archivum immunologiae et therapiae experimentalis* 2019;67:213-23.
17. Wang Y, Yang L, Li P, et al. Circulating microRNA Signatures Associated with Childhood Asthma. *Clinical laboratory* 2015;61:467-74.
18. Munitz A, Karo-Atar D, Foster PS. Asthma diagnosis: MicroRNAs to the rescue. *The Journal of allergy and clinical immunology* 2016;137:1447-8.
19. Li P, Lang X, Xia S. Elevated expression of microRNA-378 in children with asthma aggravates airway remodeling by promoting the proliferation and apoptosis resistance of airway smooth muscle cells. *Experimental and therapeutic medicine* 2019;17:1529-36.

20. Taka S, Tzani-Tzanopoulou P, Wanstall H, Papadopoulos NG. MicroRNAs in Asthma and Respiratory Infections: Identifying Common Pathways. *Allergy, asthma & immunology research* 2020;12:4-23.
21. Plank MW, Maltby S, Tay HL, et al. MicroRNA Expression Is Altered in an Ovalbumin-Induced Asthma Model and Targeting miR-155 with Antagomirs Reveals Cellular Specificity. *PloS one* 2015;10:e0144810.
22. Tang GN, Li CL, Yao Y, et al. MicroRNAs Involved in Asthma After Mesenchymal Stem Cells Treatment. *Stem cells and development* 2016;25:883-96.
23. Chen Y, Mao ZD, Shi YJ, et al. Comprehensive analysis of miRNA-mRNA-lncRNA networks in severe asthma. *Epigenomics* 2019;11:115-31.
24. Honardoost MA, Naghavian R, Ahmadinejad F, Hosseini A, Ghaedi K. Integrative computational mRNA-miRNA interaction analyses of the autoimmune-deregulated miRNAs and well-known Th17 differentiation regulators: An attempt to discover new potential miRNAs involved in Th17 differentiation. *Gene* 2015;572:153-62.
25. Woeller CF, Thatcher TH, Van Twisk D, et al. Detection of Serum microRNAs From Department of Defense Serum Repository: Correlation With Cotinine, Cytokine, and Polycyclic Aromatic Hydrocarbon Levels. *Journal of occupational and environmental medicine* 2016;58:S62-71.
26. Bai J, Zhang Z, Li X, Liu H. MicroRNA-365 inhibits growth, invasion and metastasis of malignant melanoma by targeting NRP1 expression. *Cancer biomarkers : section A of Disease markers* 2015;15:599-608.
27. Huang W-C, Jang T-H, Tung S-L, Yen T-C, Chan S-H, Wang L-H. A novel miR-365-3p/EHF/keratin 16 axis promotes oral squamous cell carcinoma metastasis, cancer stemness and drug resistance via enhancing  $\beta$ 5-integrin/c-met signaling pathway. *Journal of Experimental & Clinical Cancer Research* 2019;38.
28. Zhang S, Laryea Z, Panganiban R, Lambert K, Hsu D, Ishmael FT. Plasma microRNA profiles identify distinct clinical phenotypes in human asthmatics. *Journal of Translational Genetics and Genomics* 2018.
29. Xing Y, Fu J, Yang H, et al. MicroRNA expression profiles and target prediction in neonatal Wistar rat lungs during the development of bronchopulmonary dysplasia. *International journal of molecular medicine* 2015;36:1253-63.
30. Ha H, Debnath B, Neamati N. Role of the CXCL8-CXCR1/2 Axis in Cancer and Inflammatory Diseases. *Theranostics* 2017;7:1543-88.
31. Guyi Wang YL, Mu Yi Yang, Shaokun Liu, Libing Ma, Subo Gong, Keng Li , Li Zhang & Xudong Xiang. Effect of  $\beta$ -arrestin 2 on cytokine production of CD4+ T lymphocytes of mice with allergic asthma. *Indian Journal of Experimental Biology*;Vol.49, August 2011, pp 585-593.
32. Nichols HL, Saffeddine M, Theriot BS, et al.  $\beta$ -Arrestin-2 mediates the proinflammatory effects of proteinase-activated receptor-2 in the airway. *Proceedings of the National Academy of Sciences* 2012;109:16660-5.

## Figures

**Figure 1**

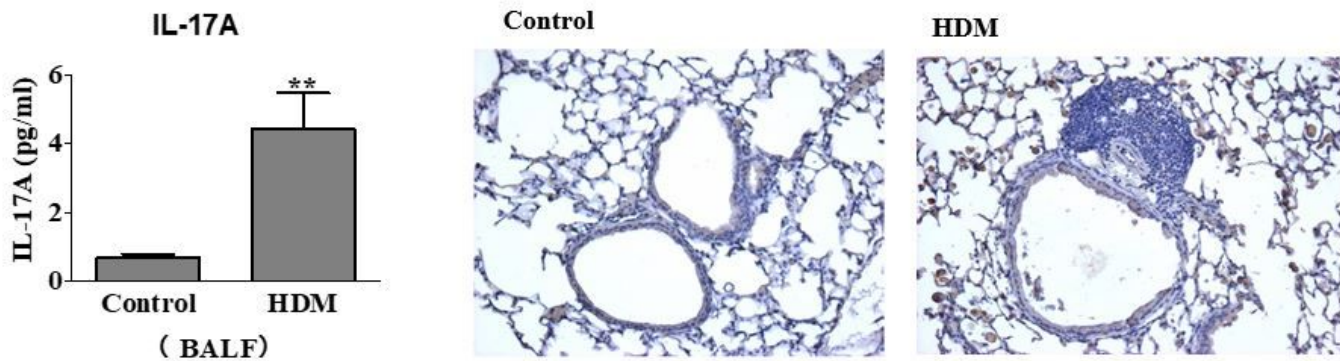


**Figure 1**

House dust mite (HDM) extract induced the production of IL-17 in severe asthma mice. A. The level of IL-17A in mouse Bronchoalveolar lavage fluid (BALF) was detected by ELISA, P<0.01. B. Immunohistochemically staining of mouse lung tissue sections, the brown area represents IL-17 positive.

**Figure 1**

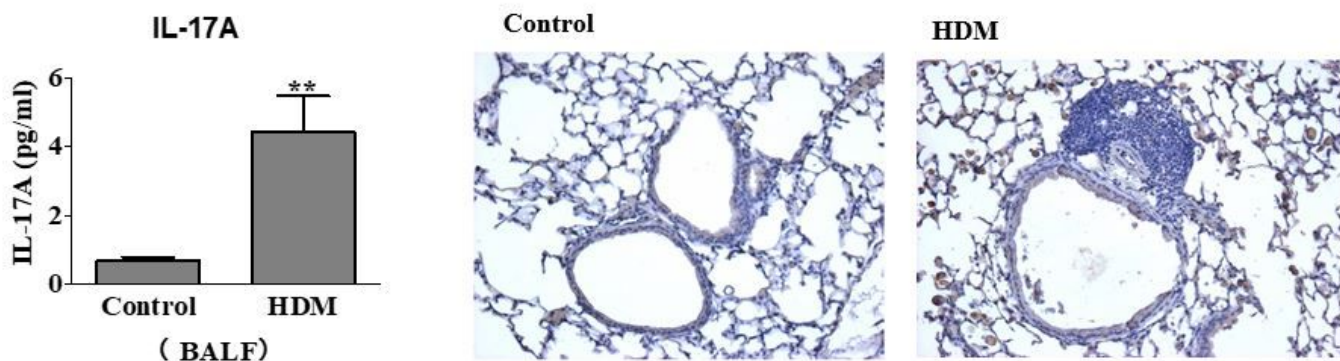
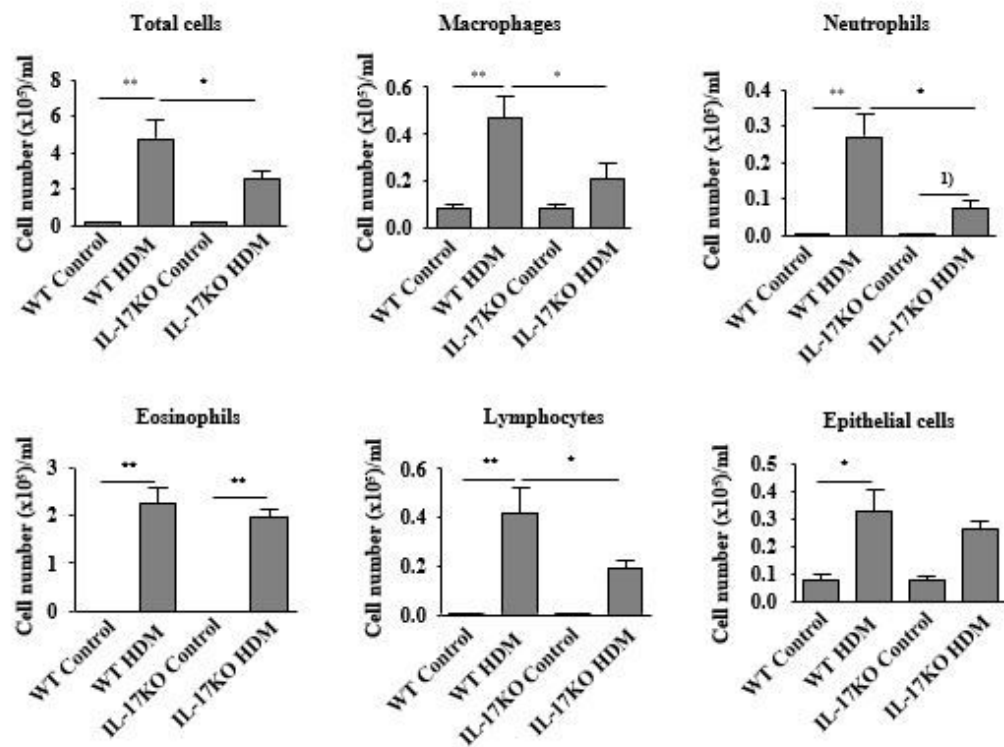


**Figure 1**

House dust mite (HDM) extract induced the production of IL-17 in severe asthma mice. A. The level of IL-17A in mouse Bronchoalveolar lavage fluid (BALF) was detected by ELISA, P<0.01. B. Immunohistochemically staining of mouse lung tissue sections, the brown area represents IL-17 positive.

A



B

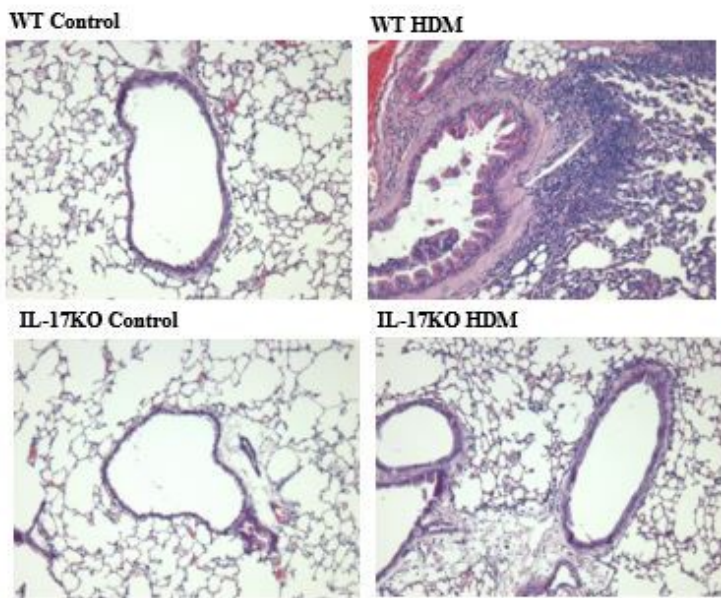
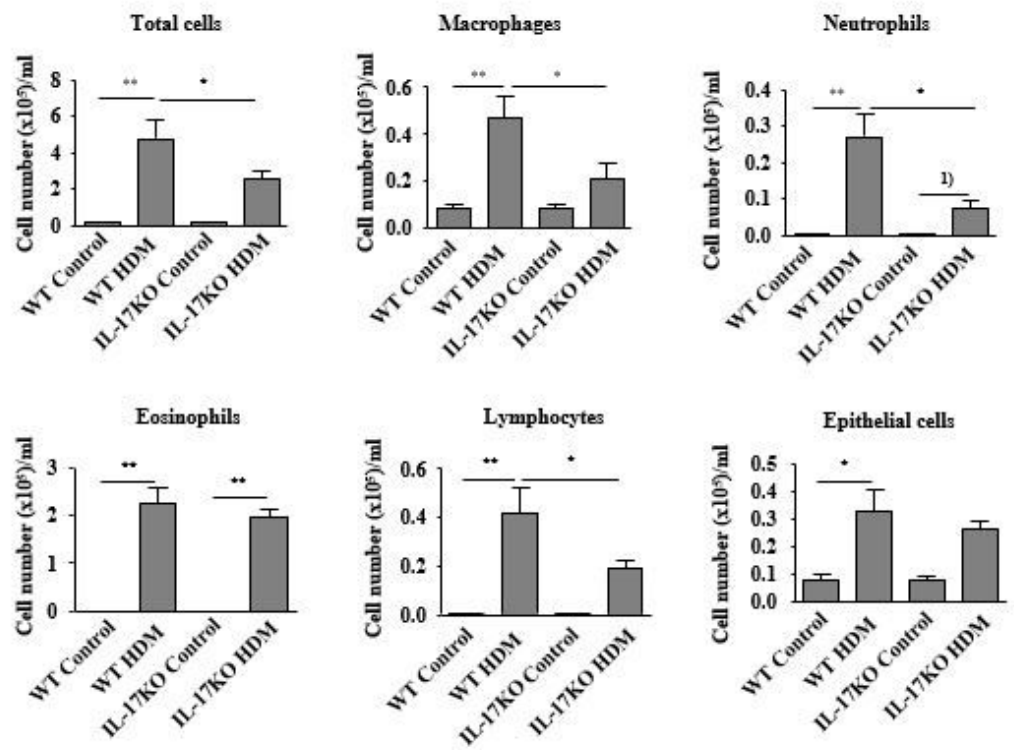


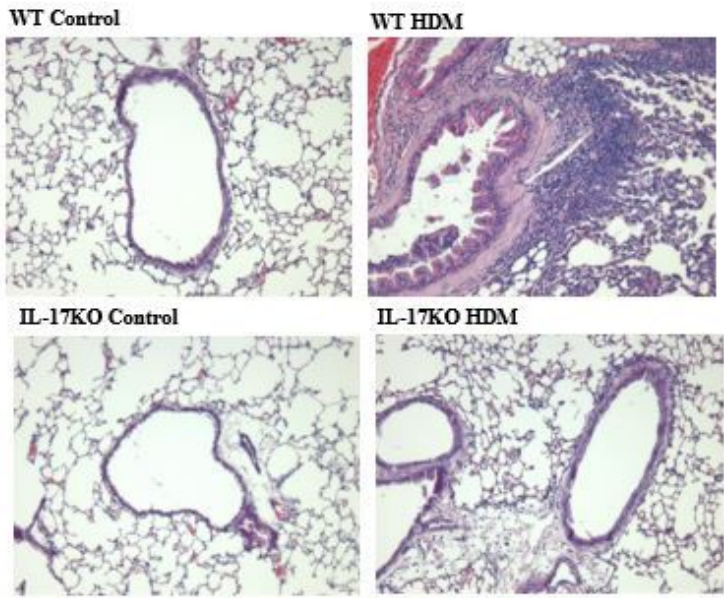
**Figure 2**

Inflammatory cell infiltration in mouse lung tissue. A. Counts of inflammatory cells in BALF. \*P<0.05, \*\*P<0.01, \*\*\*P<0.001. B. H&E staining of mouse lung tissue.

A



B

**Figure 2**

Inflammatory cell infiltration in mouse lung tissue. A. Counts of inflammatory cells in BALF. \* $P<0.05$ , \*\* $P<0.01$ , \*\*\* $P<0.001$ . B. H&E staining of mouse lung tissue.

**Figure 3**

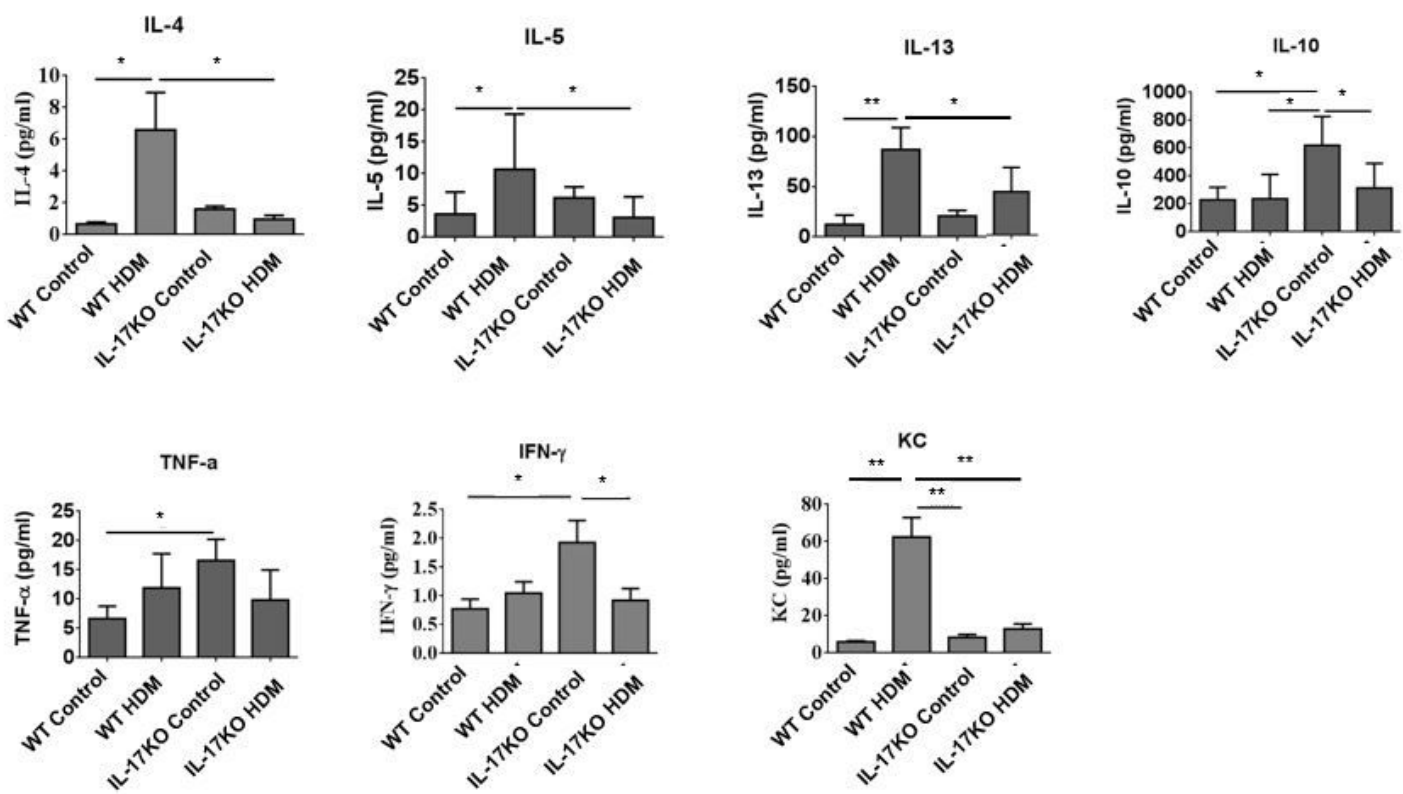


**Figure 3**

The level of inflammatory cytokines in BALF. The inflammatory cytokines in BALF were tested by ELISA.  
\*P<0.05, \*\*P<0.01.

**Figure 3**

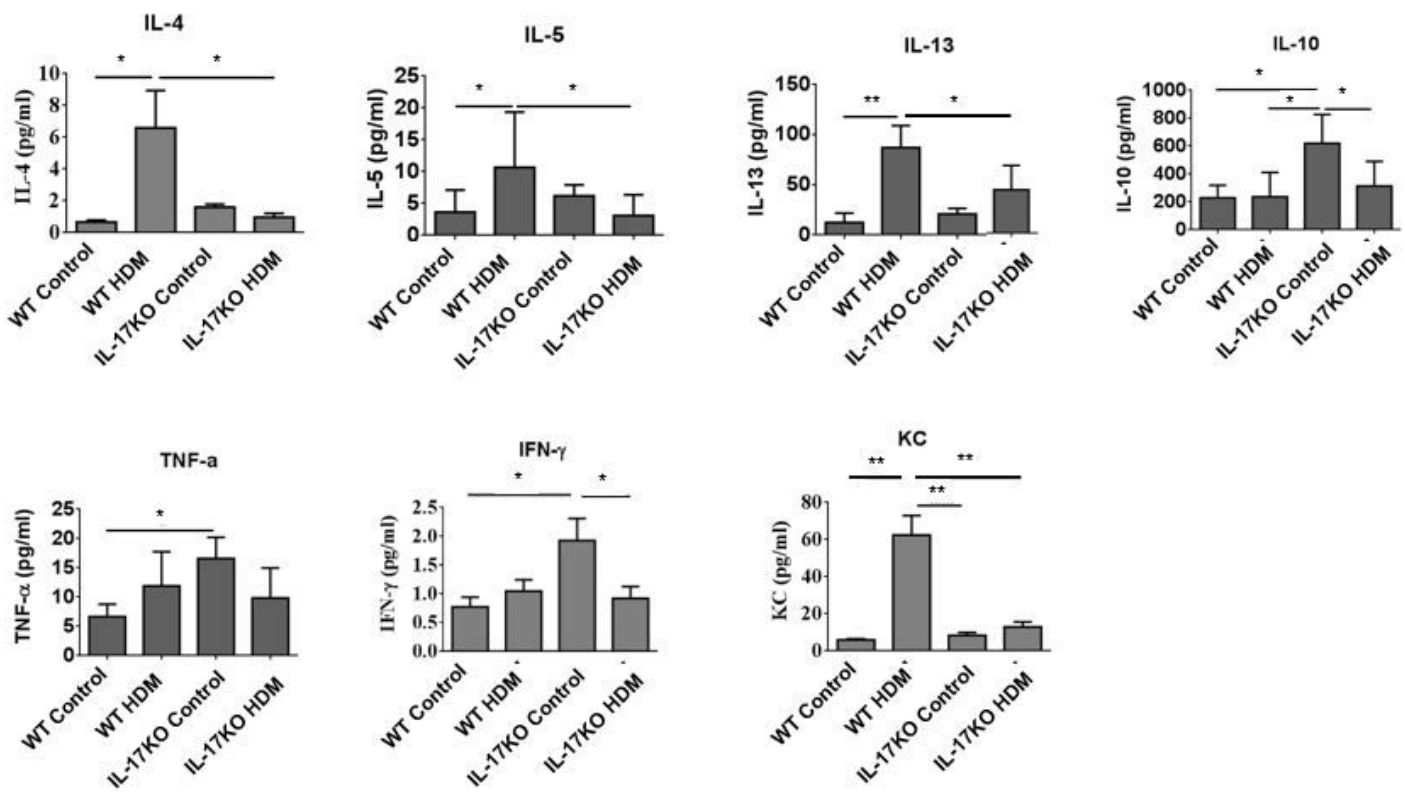
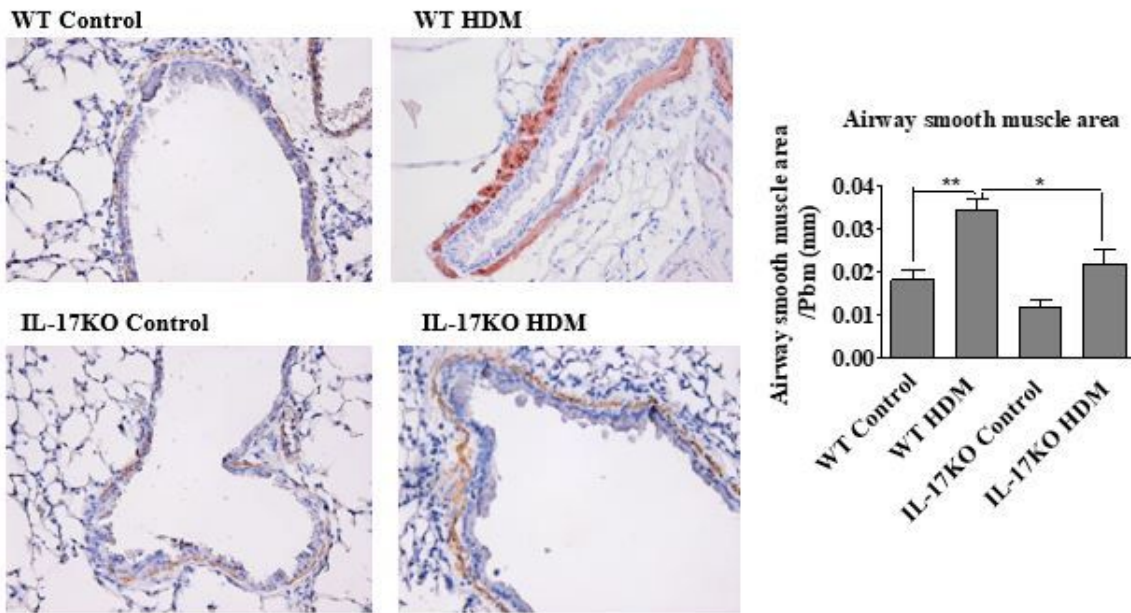


**Figure 3**

The level of inflammatory cytokines in BALF. The inflammatory cytokines in BALF were tested by ELISA.  
\*P<0.05, \*\*P<0.01.

**Figure 4**

**A**



**B**

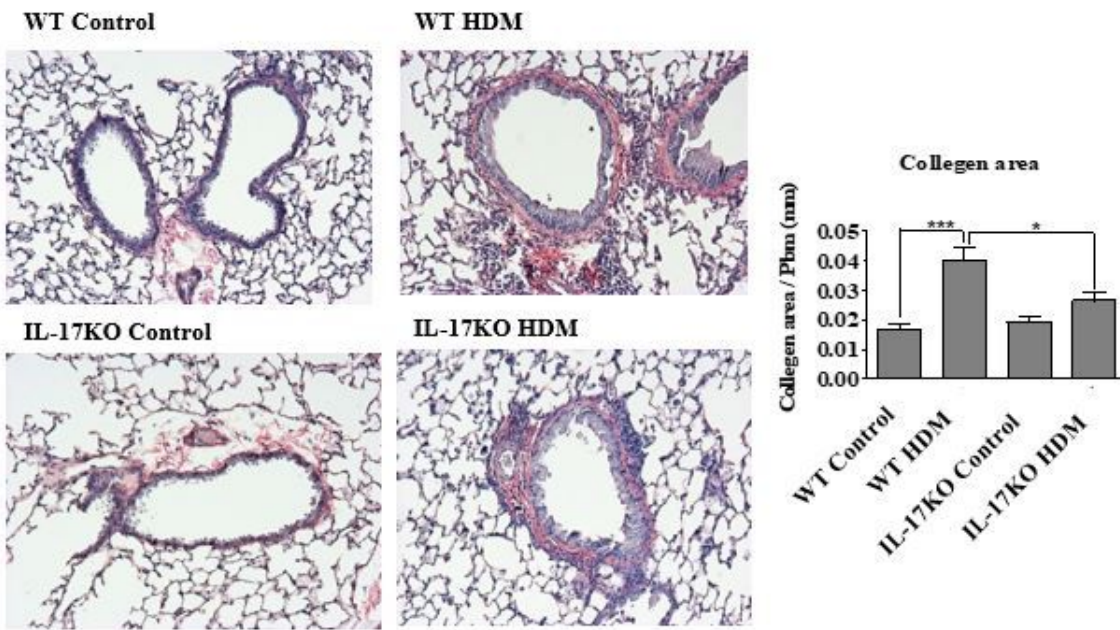
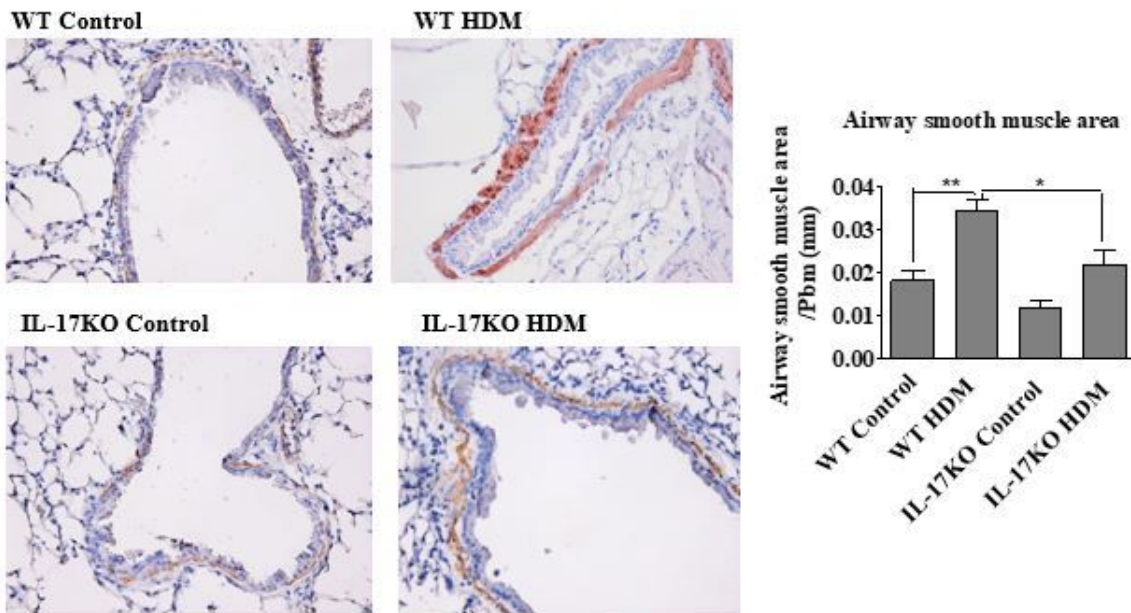


**Figure 4**

A. Airway smooth muscle mass in mouse lung tissue. Alpha-Smooth Muscle Actin was stained by immunohistochemistry. The brown areas represent the airway smooth muscle cells. \*P<0.05, \*\*P<0.01. B. Collagen deposition in mouse lung tissue. Collagen was stained by Picro Sirius red, the color red indicates the positive staining. \*P<0.05, \*\*\*P<0.001.

**Figure 4**

**A**



**B**

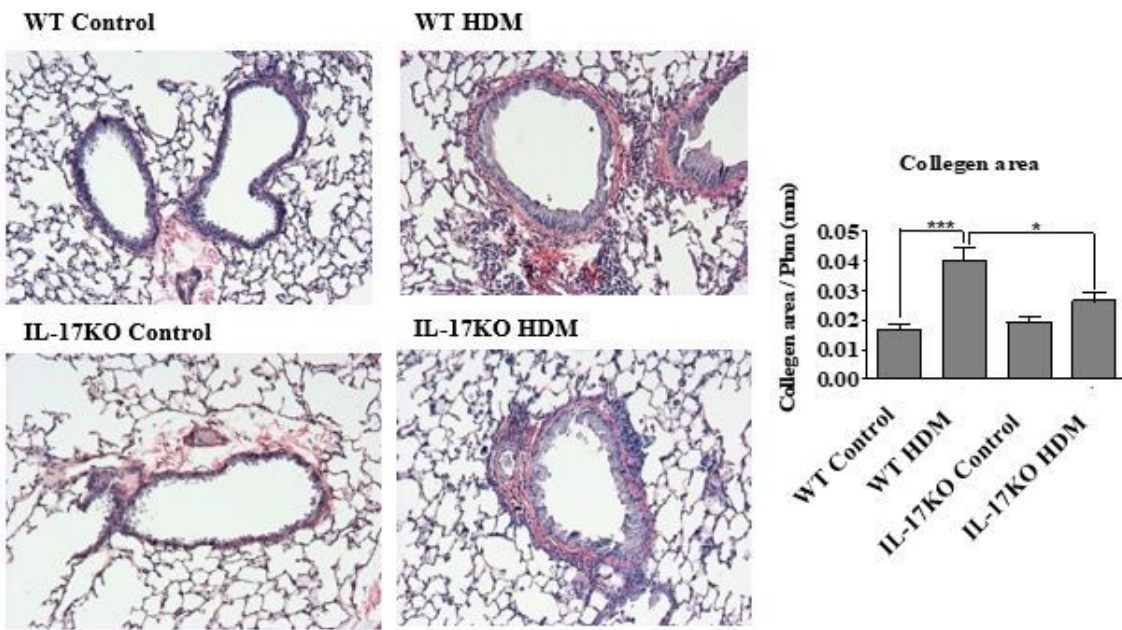


**Figure 4**

A. Airway smooth muscle mass in mouse lung tissue. Alpha-Smooth Muscle Actin was stained by immunohistochemistry. The brown areas represent the airway smooth muscle cells. \*P<0.05, \*\*P<0.01. B. Collagen deposition in mouse lung tissue. Collagen was stained by Picro Sirius red, the color red indicates the positive staining. \*P<0.05, \*\*\*P<0.001.

**Figure 5**

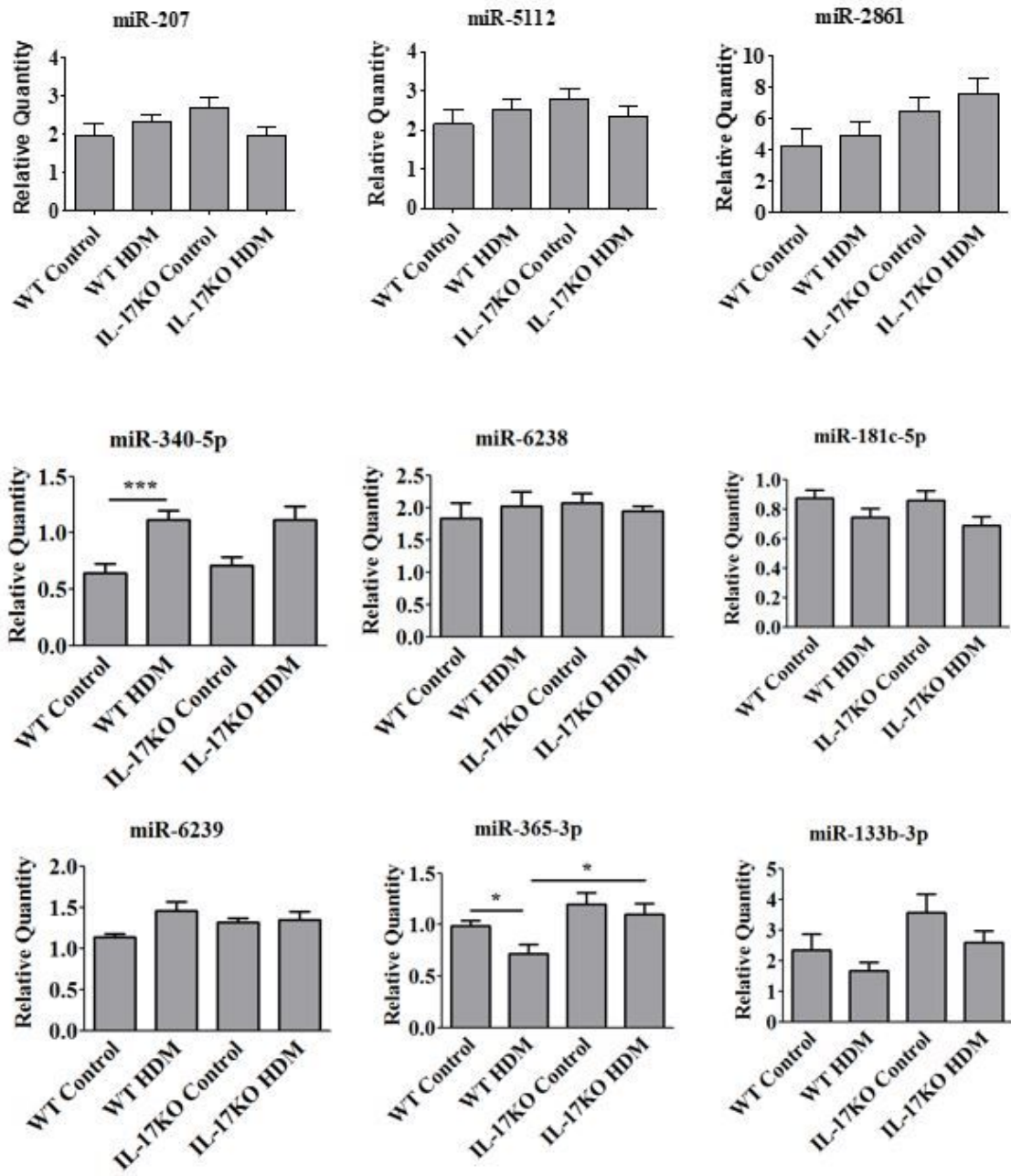


**Figure 5**

Expression of miRNAs selected from microRNA array in mouse lung tissue. The expression of miRNAs was verified by qRT-PCR. \*P<0.05, \*\*P<0.01, \*\*\*P<0.001.

**Figure 5**

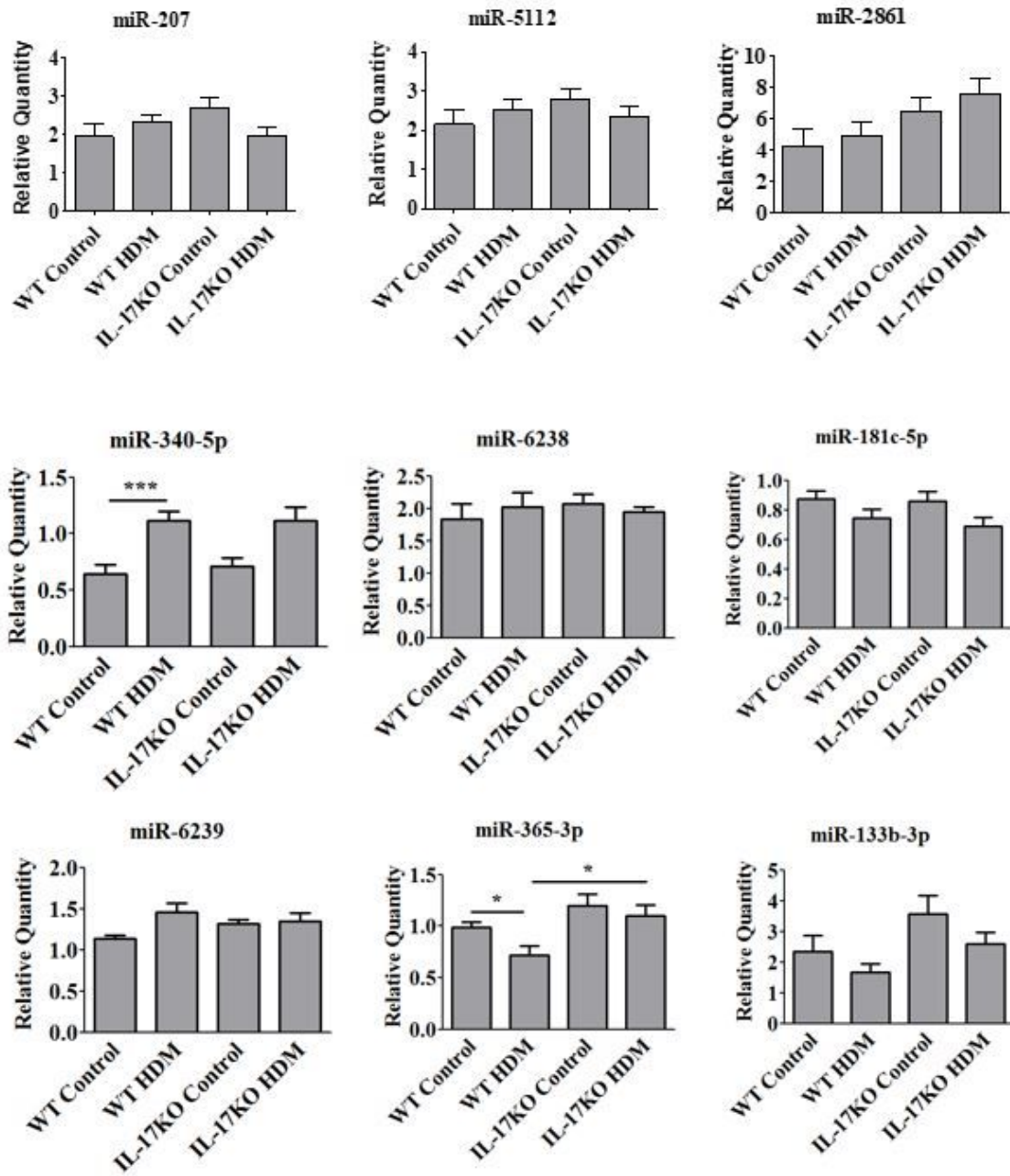
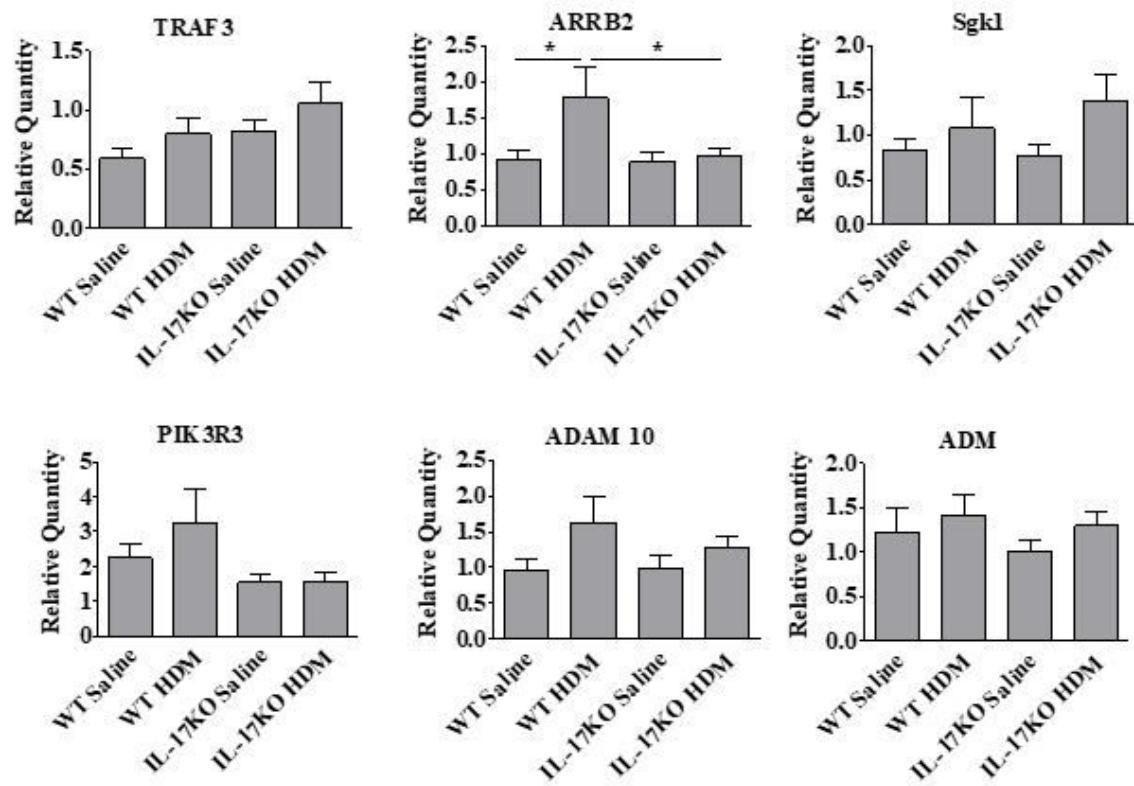


**Figure 5**

Expression of miRNAs selected from microRNA array in mouse lung tissue. The expression of miRNAs was verified by qRT-PCR. \*P<0.05, \*\*P<0.01, \*\*\*P<0.001.

**Figure 6**

**A**



**B**

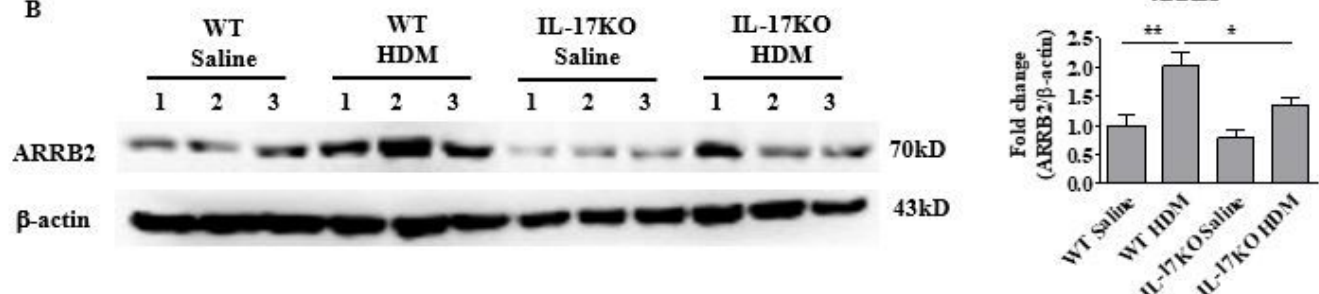
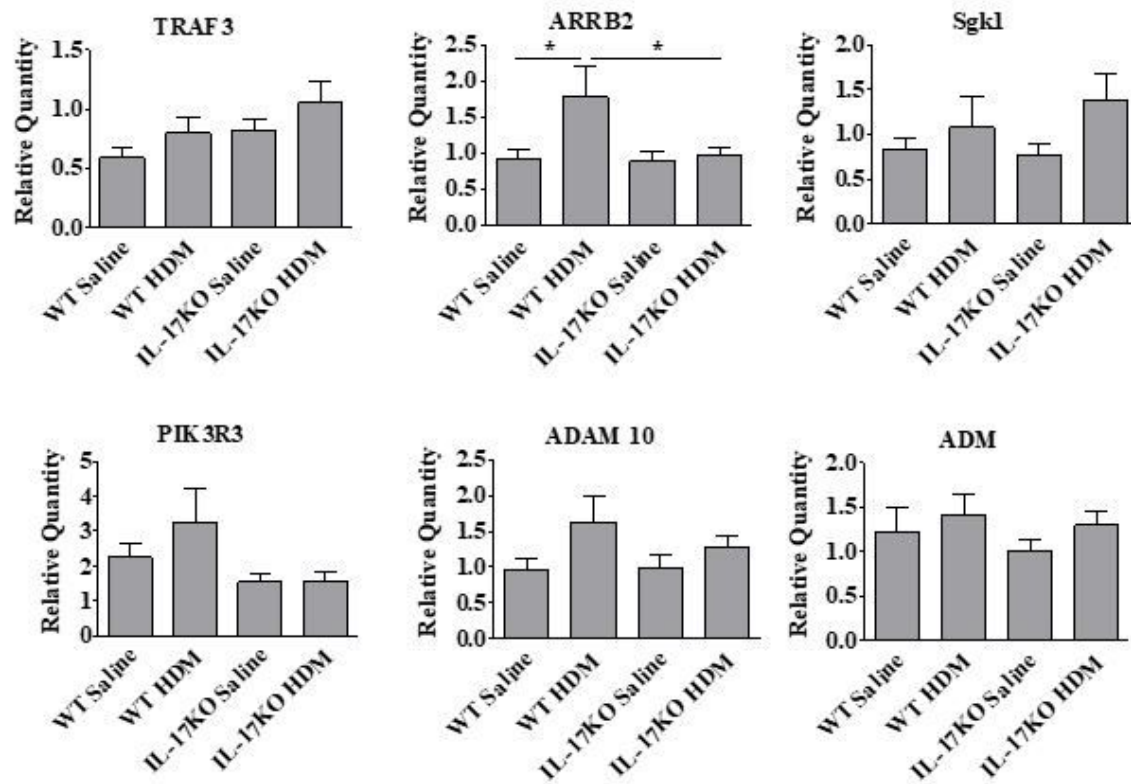


**Figure 6**

Expression of predicted target genes of miR-365-3p in mouse lung tissue. A. mRNA expression of predicted target genes was detected by qRT-PCR \*P<0.05. B. Expression of ARRB2 protein was detected by western-blot. \*P<0.05, \*\*P<0.01.

**Figure 6**

**A**



**B**

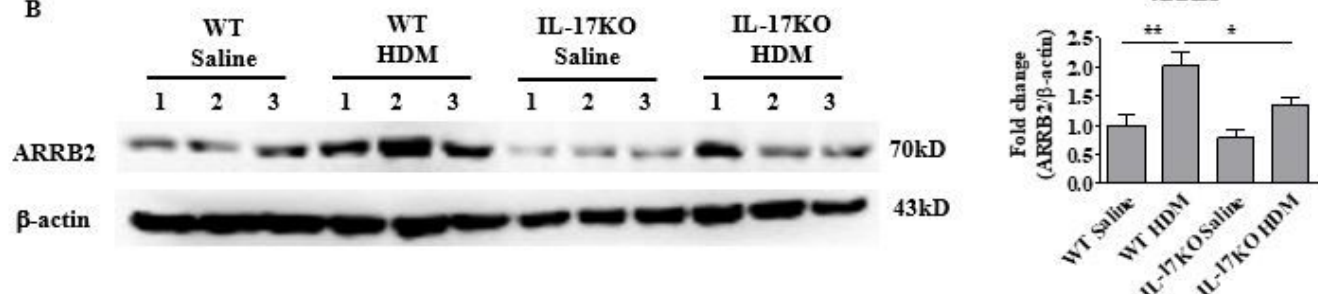


**Figure 6**

Expression of predicted target genes of miR-365-3p in mouse lung tissue. A. mRNA expression of predicted target genes was detected by qRT-PCR \*P<0.05. B. Expression of ARRB2 protein was detected by western-blot. \*P<0.05, \*\*P<0.01.

**Figure 7**

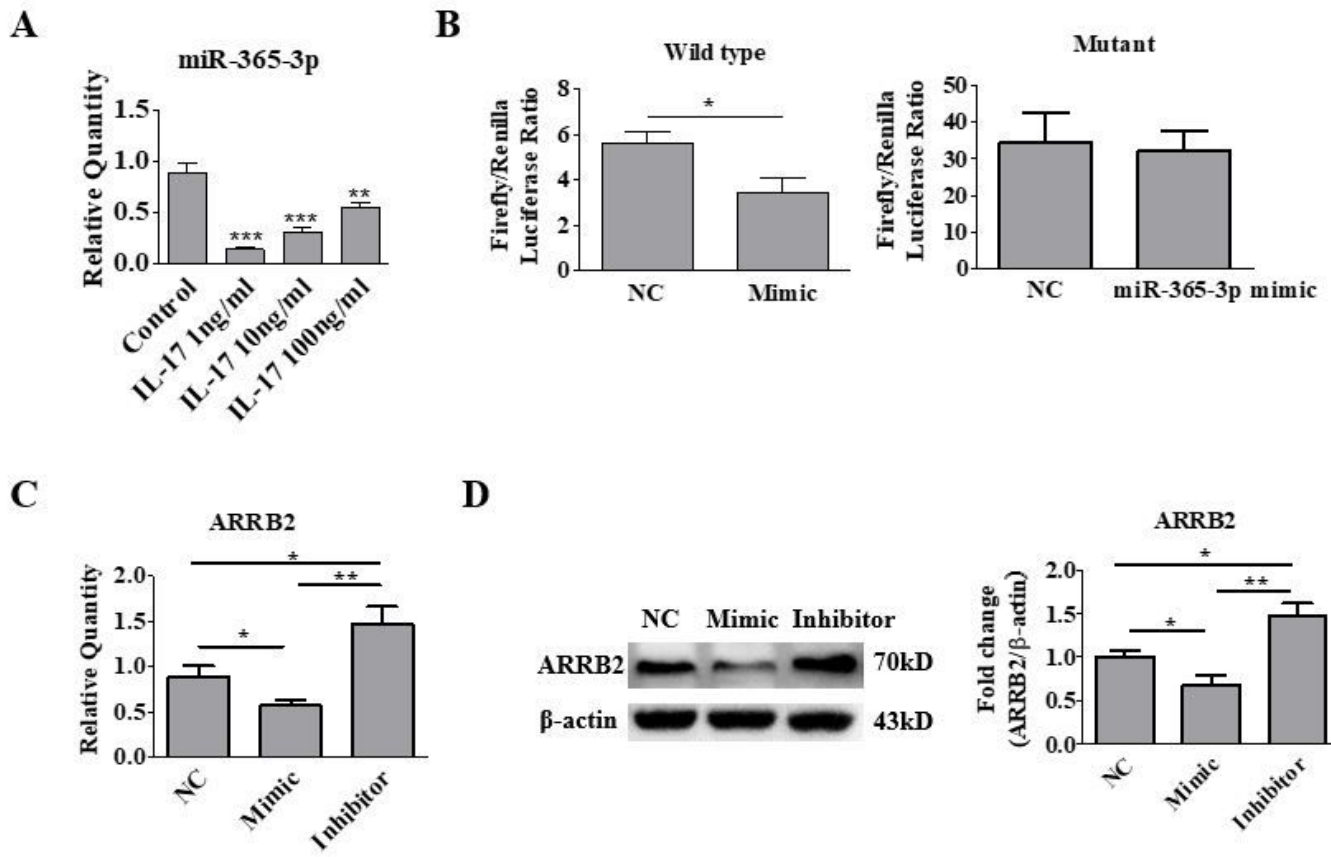


**Figure 7**

The regulatory role of miR-365-3p in mouse alveolar epithelial (MLE-12) cells. A. The effect of IL-17 in miR-365-3p expression in MLE-12 cells. The MLE-12 cells were treated by IL-17 in different concentrations (1ng/ml, 10ng/ml and 100ng/ml), and the miR-365-3p expression was tested by qRT-PCR \*P<0.05, \*\*P<0.01, \*\*\*P<0.001, N=4. B. The targeting role of miR-365-3p on ARRB2 was examined by reporter fluorescence assays, \*P<0.05, N=3. C. Effect of miR-365-3p mimic and inhibitor on mRNA level of ARRB2, \*P<0.05, \*\*P<0.01, N=6. D. Effect of miR-365-3p mimic and inhibitor on protein level of ARRB2, \*P<0.05, \*\*P<0.01, N=6.

**Figure 7**

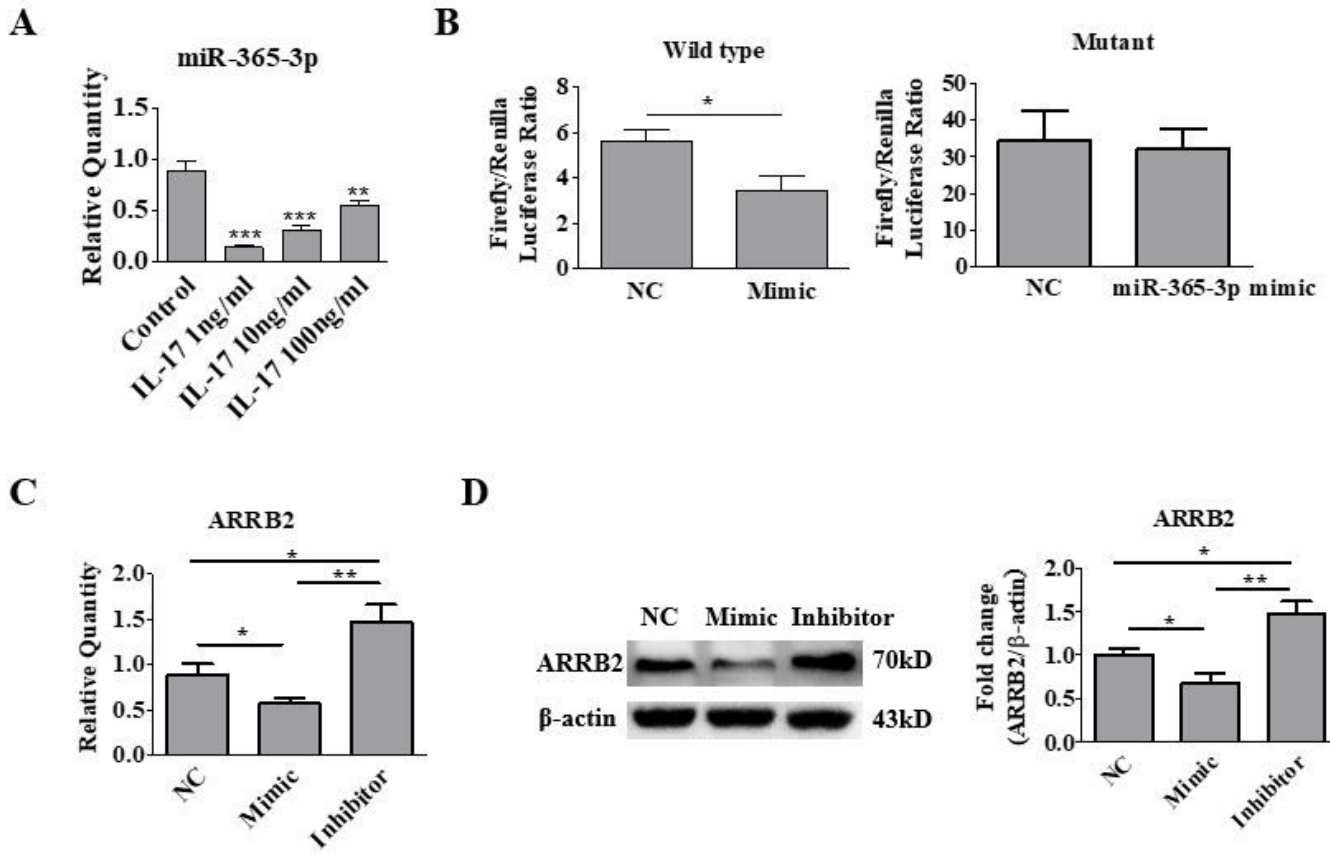


**Figure 7**

The regulatory role of miR-365-3p in mouse alveolar epithelial (MLE-12) cells. A. The effect of IL-17 in miR-365-3p expression in MLE-12 cells. The MLE-12 cells were treated by IL-17 in different concentrations (1ng/ml, 10ng/ml and 100ng/ml), and the miR-365-3p expression was tested by qRT-PCR \*P<0.05, \*\*P<0.01, \*\*\*P<0.001, N=4. B. The targeting role of miR-365-3p on ARRB2 was examined by reporter fluorescence assays, \*P<0.05, N=3. C. Effect of miR-365-3p mimic and inhibitor on mRNA level of ARRB2, \*P<0.05, \*\*P<0.01, N=6. D. Effect of miR-365-3p mimic and inhibitor on protein level of ARRB2, \*P<0.05, \*\*P<0.01, N=6.